Int. J. Heat Mass Transfer. Vol. 11, pp. 1675–1693. Pergamon Press 1968. Printed in Great Britain

LAMINAR NATURAL CONVECTION IN AN ENCLOSED RECTANGULAR CAVITY

G. DE VAHL DAVIS*

(*Received* 22 *April* 1968)

Abstract—A study is described of the steady laminar two dimensional motion of a fluid in an enclosed cavity, the motion being generated by a temperature gradient normal to the direction of the body force. The governing equations have been solved numerically. The results are compatible with, and form an extension of, some previous theoretical and experimental results. Maximum values considered of the Rayleigh number (based on cavity height) were 2×10^5 for a square cavity and $1{\cdot}25 \times 10^6$ for one of height/thickness ratio = 5. Some new details of the flow at high Rayleigh numbers have been revealed. It has been found that high Prandtl numbers exert a stabilizing influence on the numerical solution, while they have only a small effect on the final results (over the range $10^{-1} \leqslant Pr \leqslant 10^3$).

NOMENCLATURE

d, cavity width;
g, acceleration due to gravity;
l, cavity height;
p, fluid pressure;
Pr, Prandtl number, ν/α;
Ra, Rayleigh number, $\beta g d^3(T_h - T_c)/\alpha\nu$;
T, fluid temperature;
T_c, T_h, temperatures of cold, hot wall of cavity;
u, v, velocity components in the x, y directions;
x', y', dimensional coordinates (Fig. 1);
x, y, dimensionless coordinates ($x = x'/d$; $y = y'/d$).

Greek symbols

α, fluid thermal diffusivity;
β, coefficient of cubical expansion;
θ, dimensionless temperature, $(T - T_c)/(T_h - T_c)$;
ν, fluid kinematic viscosity;
ρ, fluid density;
ψ, dimensionless stream function.

* School of Mechanical Engineering, University of New South Wales, Kensington, N.S.W., 2033, Australia.

INTRODUCTION

THE PROBLEM to be considered is that of the motion which occurs when a fluid is contained in a cavity, the surfaces of which are non-uniform in temperature. Specifically, attention will be given to a rectangular cavity as shown in Fig. 1. Motion occurs because the walls $y' = 0$ and $y' = d$ are at different temperatures.

It is supposed that the cavity is sufficiently long in the direction normal to the plane of Fig. 1 for the motion to be assumed to be two-dimensional. It will further be assumed that the motion is laminar. Experimental evidence (e.g. [1] and [14]) indicates that this assumption is valid provided the Rayleigh number based on cavity height is less than about 10^8.

The motivation for a study of this problem arises typically from situations in which the insulating value of such a cavity is of interest. Among these are such diverse applications as a double-glazed window and a gas-filled cavity surrounding a nuclear reactor core. The problem is, moreover, of intrinsic interest since its mathematical description leads to a set of non-linear partial differential equations the solution of which, even in numerical form, poses a formidable challenge. Attention to these types of equations has been increasing of late, so that

a growing class of engineering problems is becoming subject to successful theoretical attack.

Typically, in the kinds of application mentioned, the height of the cavity would be much greater than its width, with l/d of the order of 10–50. In the present study, however, attention has so far been directed primarily to square cavities; a few results have been obtained for $l/d = 5$. Analytically, this problem is more difficult; a large l/d permits a boundary-layer approximation to be made, enabling some useful results [1] to be obtained. Computationally, however, it is somewhat less complicated, largely because the number of mesh points required is smaller.

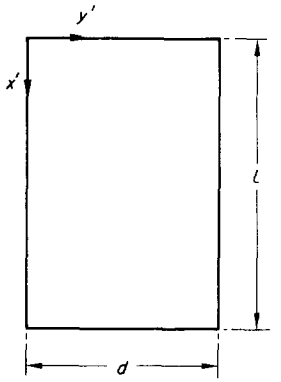

FIG. 1. Rectangular cavity notation.

PREVIOUS WORK

The chronicle of analytical attacks on this problem starts with Batchelor's paper [2], although considerable attention had been (and is still being) given to the analogous problem of the so-called Bénard cell, viz. convection in a fluid confined between two *horizontal* boundaries.* Batchelor's attention was motivated by an interest in the thermal insulation of buildings, in particular by double-glazed windows. He therefore limited his attention to large values of l/d, except for an attempt at a series solution, which proved to be useful only for very small values of Ra (considerably less than 1000) as the series were very slowly convergent.

With a characteristic mixture of analysis and intuition, Batchelor obtained estimates of the Nusselt number in what are now called the conduction and transition regimes of flow, and of a criterion for the change from one regime to the other. He also concluded that, at sufficiently high Rayleigh numbers, the flow would consist of a core, of constant temperature and vorticity, surrounded by a continuous boundary layer. The results to be presented here show a trend, at the maximum Rayleigh numbers, towards a core of approximately constant vorticity but not of constant temperature.

The first attempt to obtain a numerical solution of the relevant equations was made by Poots [4], who used a double series of orthogonal functions to represent each of the variables ψ (stream function) and θ (temperature). A doubly-infinite set of coupled simultaneous algebraic equations for the coefficients was obtained and solved (to an accuracy of about four significant figures) for five values of Rayleigh number. The computations were performed by hand. For four values of $Ra \leqslant 5000$, the agreement between the values of Nusselt number obtained by Poots with those found here is excellent. At $Ra \leqslant 10000$ his value is 3 per cent less than ours.

A related problem—that of natural convection through a fluid contained in a long horizontal cylinder of non-uniform wall temperature—has been studied by Hellums and Churchill [5]. After making certain simplifications in the governing equations, numerical solutions were obtained which were in fair agreement with some experimental data of Martini and Churchill [6]. The discrepancies, beyond those due to experimental uncertainty, were attributed by Hellums and Churchill to (a) the neglect of the temperature dependence of physical properties in the computations, (b) the neglect of the radial momentum balance in the computations and

* In Bénard's experiments [3], a layer of volatile liquid with a free surface was cooled from above by evaporation. Although the ensuing motion was originally attributed to thermal instability, it is now generally believed that surface tension effects were predominant. However, Bénard's name seems firmly linked to the thermal problem.

(c) a simplification of the experimental boundary conditions made in the mathematical model.

Convection in a horizontal cylinder has been treated analytically by several authors. A publication by Menold and Ostrach [7], for example, is concerned with the case in which the Rayleigh and Prandtl numbers are large, and the Grashof number is of unit order. This report contains a comprehensive bibliography.

The method of solution used by Hellums and Churchill was subsequently employed by Wilkes and Churchill [8] on the present (rectangular cavity) problem. This method seeks the steady temperature and stream function distribution by solving the initial value problem of a fluid, initially at rest in an isothermal cavity, which is suddenly subjected to the desired thermal boundary condition. This method has the attraction that it yields information on the transient conditions which exist prior to the establishment of a steady state. On the other hand it is subject to stability difficulties which limited Wilkes to a Rayleigh number of about 75000 (with Ra defined as below). Indeed even this solution, while satisfying the finite difference approximations, is not physically acceptable (as discussed by Wilkes [9]). The difficulty apparently arises from the fact that vorticity was retained explicitly as one of the unknowns, when boundary conditions for it cannot be obtained *ab initio*. It was necessary to compute the vorticity at the boundary from the stream function distribution near the boundary as the calculations proceeded.

A numerical study has been made by Aziz [10] of both the two- and three-dimensional motion in a fluid heated from below. Steady solutions were obtained for Rayleigh numbers up to 3500. The unsteady equations were again employed, but the transient solution is of little interest as it depended on the disturbance introduced to initiate the motion of the fluid. This appears to be the first detailed solution of the full equations of motion and energy in three dimensions.

A paper on the present topic has been published by Elder [11]. An iterative procedure was used to solve the steady equations, which were decomposed into a set of five of the second order by the introduction of vorticity and the rates of generation of vorticity and temperature as variables, in addition to ψ and θ. Boundary condition problems were again encountered; numerical stability was achieved by requiring the normal gradient of the vorticity to vanish on the horizontal boundaries of the cavity. This arbitrary condition (which has no physical justification) was claimed to affect only the end regions. However, since all the results (with one exception) are for a square cavity, the effect of the condition is to place those results in some doubt.

Some preliminary results of the present study were published by de Vahl Davis and Kettleborough [12]. They were obtained on an "old" English Electric Deuce computer, and because of capacity and speed limitations were limited to low Rayleigh numbers and very coarse meshes. The method used then and, with some useful modifications, in the present work is in one sense similar to that of Wilkes and Churchill. It is iterative, and successive iterates behave somewhat in the same manner as the transient solution at large times. However, no attempt has been made here to find the transient solution, and an ability to take action which can ensure stability is thereby obtained. Furthermore, the fluid vorticity has not been retained as a variable, so that their boundary conditions problem does not arise.

FORMULATION OF THE PROBLEM

Let the temperatures of the vertical walls $y' = 0$ and $y' = d$ be T_c and T_h respectively. It is assumed that $(T_h - T_c)$ is sufficiently small with respect to T_c that the Boussinesq approximation may be made, which neglects density variation in inertial terms of the equation of motion but retains it in the buoyancy term of the vertical equation. It is further assumed that all other relevant thermodynamic and transport properties are independent of temperature, and that

compressibility and dissipation effects are negligible.

The equations expressing conservation of mass, momentum and energy are then

$$\frac{\partial u}{\partial x'} + \frac{\partial v}{\partial y'} = 0 \tag{1}$$

$$u\frac{\partial u}{\partial x'} + v\frac{\partial u}{\partial y'} = -\frac{1}{\rho_0}\frac{\partial p}{\partial x'} + g\frac{\rho - \rho_0}{\rho_0} + \nu\nabla^2 u \tag{2a}$$

$$u\frac{\partial v}{\partial x'} + v\frac{\partial v}{\partial y'} = -\frac{1}{\rho_0}\frac{\partial p}{\partial y'} + \nu\nabla^2 v \tag{2b}$$

$$u\frac{\partial T}{\partial x} + v\frac{\partial T}{\partial y} = \alpha\nabla^2 T. \tag{3}$$

Consistent with the previous assumptions, the density is given by

$$\frac{\mathrm{d}\rho}{\rho_0} = -\beta\,\mathrm{d}T. \tag{4}$$

The subscript in (2) and (4) denotes a reference state, say that at the cold wall temperature T_c.

The following dimensionless variables are introduced:

$$x = x'/d; \qquad y = y'/d; \qquad \theta = \frac{T - T_c}{T_h - T_c};$$

and, consistent with (1), a dimensionless stream function ψ is defined by

$$u = \frac{\alpha}{d}\frac{\partial \psi}{\partial y}, \qquad v = -\frac{\alpha}{d}\frac{\partial \psi}{\partial x}.$$

Then, combining (2a) and (2b) to eliminate pressure, and making use of (1), we obtain

$$\nabla^4\psi = \frac{1}{Pr}\left\{\frac{\partial(\nabla^2\psi, \psi)}{\partial(x, y)}\right\} + Ra\frac{\partial\theta}{\partial y} \tag{5}$$

and

$$\nabla^2\theta = \frac{\partial(\theta, \psi)}{\partial(x, y)} \tag{6}$$

where $Pr = \nu/\alpha$, the Prandtl number, and

$$Ra = \frac{\beta(T_h - T_c)gd^3}{\alpha\nu}, \text{ the Rayleigh number.}$$

Equations (5) and (6) are subject to the conditions that ψ and its first derivatives vanish at the boundaries, and that θ or its normal derivative are specified at the boundaries. The method of solution is unaffected by the prescription on θ. We have considered here

at $x = 0$ and $x = l/d$:

$$\psi = \partial\psi/\partial x = 0, \quad \theta = y \tag{7a}$$

or

at $x = 0$ and $x = l/d$:

$$\psi = \partial\psi/\partial x = \partial\theta/\partial x = 0 \tag{7b}$$

and

at $y = 0$ and $y = 1$:

$$\psi = \partial\psi/\partial y = 0, \quad \theta = y. \tag{7c}$$

Equation (7a) describes a horizontal boundary which is a very good conductor of heat, in relation to the fluid; its temperature varies linearly across the cavity. Equation (7b) describes a boundary which is adiabatic.

NUMERICAL SOLUTION OF THE EQUATIONS

Equations (5) and (6) have been solved at the nodes of a rectangular mesh which is supposed to occupy the cavity. Full details of the method will be found in [13]; a brief description is given in the Appendix. The main steps of the numerical procedure, which is iterative, are:

1. Commencing with a given, approximate set of values of ψ and θ at the mesh points, the right-hand side of (5) is evaluated, using central finite difference approximations in place of derivatives.
2. Equation (5) is then representative of a set of equations for new values of ψ at all mesh points, and is solved.
3. Using the new ψ field and the original θ field, a finite difference approximation to the right-hand side of (6) is evaluated.

4. Equation (6) is then solved to yield a new θ field.
5. If the new ψ and θ fields are not sufficiently close to the previous fields, the process from step 1 is repeated.

It will be noticed that (6) is linear in θ: it can (for a given ψ field) be solved exactly. The same is not true for ψ in (5); the result of step 2 is not normally a solution of (5) for ψ (for a given θ field). Hence it is desirable to construct an inner iteration loop, involving steps 1 and 2 alone. Because the convergence of this loop is relatively slow, and because normally the θ values will not be correct, it is both unnecessary and undesirable to repeat the inner iteration more than a few times. In other words, a much weaker convergence criterion is used for the inner iteration.

The calculations were carried out using an 11×11 mesh, i.e. the cell size was $l/10 \times d/10$. Wilkes [9] showed that the use of a finer mesh made relatively little difference to the final results. More recent computations by Thomas [17] on natural convection between concentric cylinders have confirmed this. It is possible that the use of a finer mesh could reveal secondary flows in two corner regions. The effects of such flows on the overall heat-transfer rates would be expected to be small.

Two computers were used to carry out the computations, a CDC6600 and IBM360/50. The time necessary to obtain a solution for a particular set of conditions depended strongly, of course, on the starting values assumed for ψ and θ. The solution obtained for each Ra was used as a first approximation to the solution for the next (higher) Ra.

RESULTS

Calculations have been made for Rayleigh numbers (based on d) up to 2×10^5 and Prandtl numbers in the range 10^{-1} to 10^3; for cavities of height/spacing ratio in the range 1–5; for both linear and adiabatic boundary conditions on θ; and using 3-, 5- and 7-point central difference approximations.* (Not all possible combinations have been investigated.)

Some of the graphs which are reproduced here were prepared by the line printer of the computer. The figures need stretching for non-square cavities. In all cases the cooler wall is on the left of the figure. The magnitude of the quantity for which a given contour "band" has been printed is proportional (to the nearest 10 per cent) to the number used to display the band. For clarity, alternate bands have been left blank.

Some differences in detail arise from the use of the various finite difference approximations. As discussed in [13], the 3-point approximation is probably the most accurate, but the principal features of the flow remain the same for the three cases. In the illustrations which follow, the abbreviations 3-pt, 5-pt, or 7-pt will denote the approximation used, and the terms "linear" or "insulated" will describe the thermal condition on the horizontal boundaries.

(a) *Streamlines and isothermals*

Figures 2 and 3 show a series of streamline and isotherm distributions in a square cavity for a range of Rayleigh numbers. The development of the motion, and the accompanying distortion of the temperature distribution from that due to conduction alone, can be seen.

Figure 4 shows some corresponding information for a cavity of $l/d = 5$.

(b) *Velocity distribution*

Figure 5 shows typical contour maps of the vertical and horizontal velocity components in the cavity, and Fig. 6 shows the local speed $(u^2 + v^2)^{\frac{1}{2}}$.

More detailed information on velocities than can be obtained from the contour maps is shown in Fig. 7. The development of a boundary layer, as Ra increases, is clearly demonstrated. Of particular interest is the reverse flow which occurs near the centre of the cavity at high

* A convenient catalogue of finite difference approximations has been provided by Bickley [18].

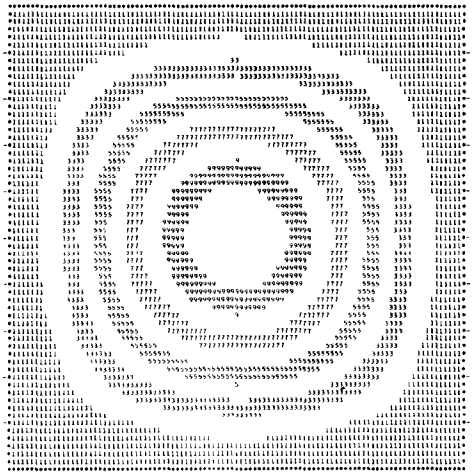

(a)(i)

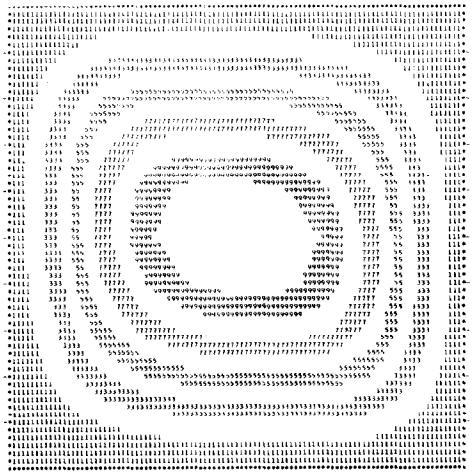

(a)(ii)

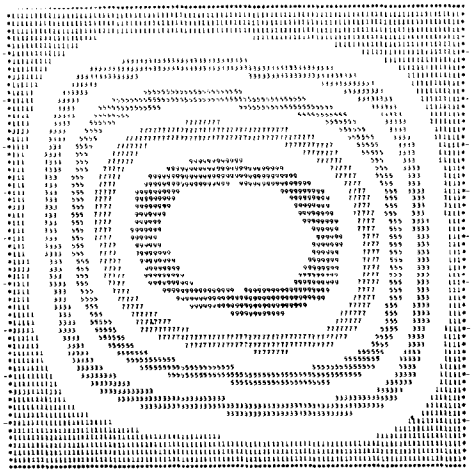

(b)(i)

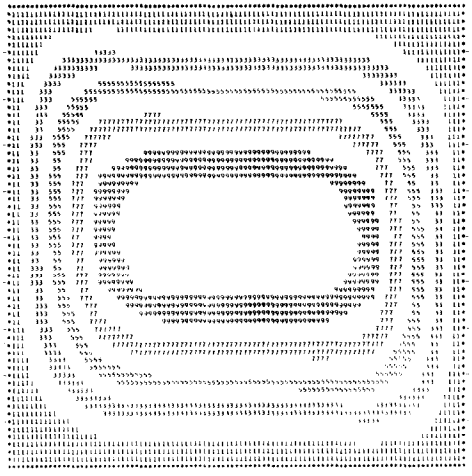

(b)(ii)

FIG. 2. Contour maps of typical stream function distributions. $l/d = 1$. (a) Linear; (i) $Ra = 10^3$, $Pr = 10$. (ii) $Ra = 2 \times 10^4$, $Pr = 10^3$. (b) Insulated; (i) $Ra = 1{\cdot}2 \times 10^4$, $Pr = 10^3$ (ii) $Ra = 5 \times 10^4$, $Pr = 10^3$.

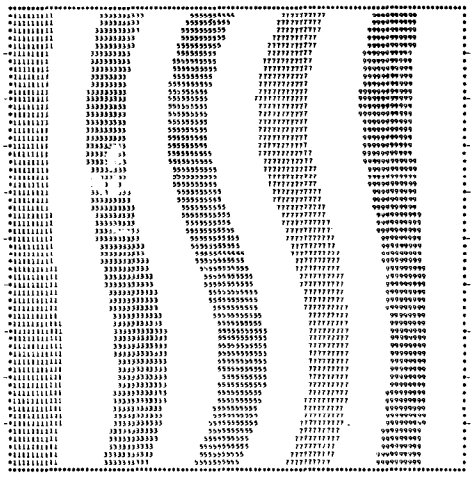

(a) (i)

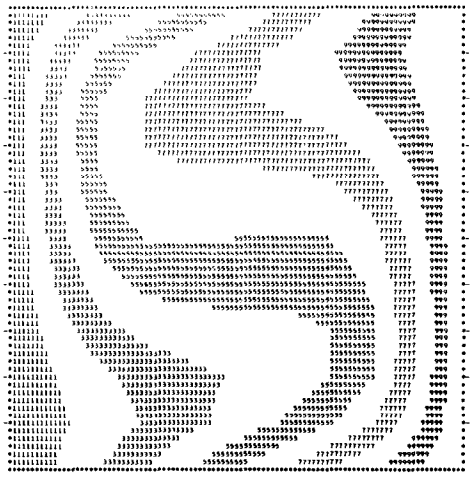

(a) (ii)

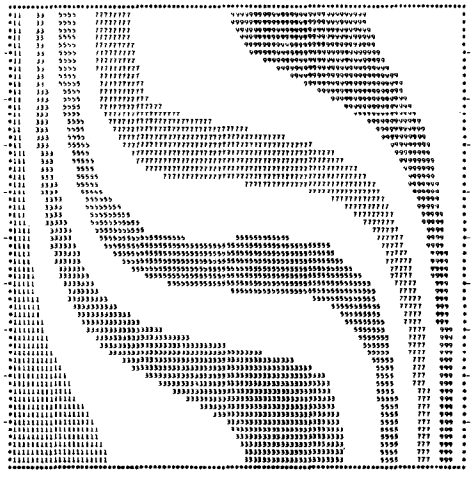

(b) (i)

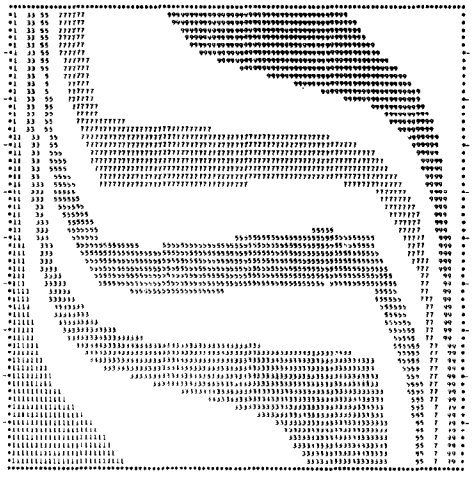

(b) (ii)

FIG. 3. Contour maps of typical isotherm distributions. $l/d = 1$. (a) Linear; (i) $Ra = 10^3$, $Pr = 10$. (ii) $Ra = 2 \times 10^4$, $Pr = 10^3$. (b) Insulated; (i) $Ra = 1{\cdot}2 \times 10^4$, $Pr = 10^3$ (ii) $Ra = 5 \times 10^4$, $Pr = 10^3$.

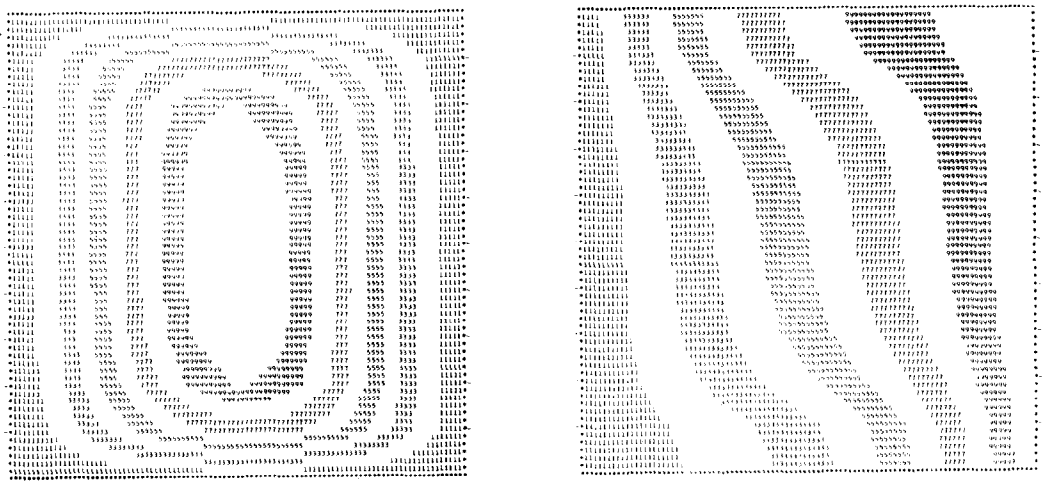

(a)

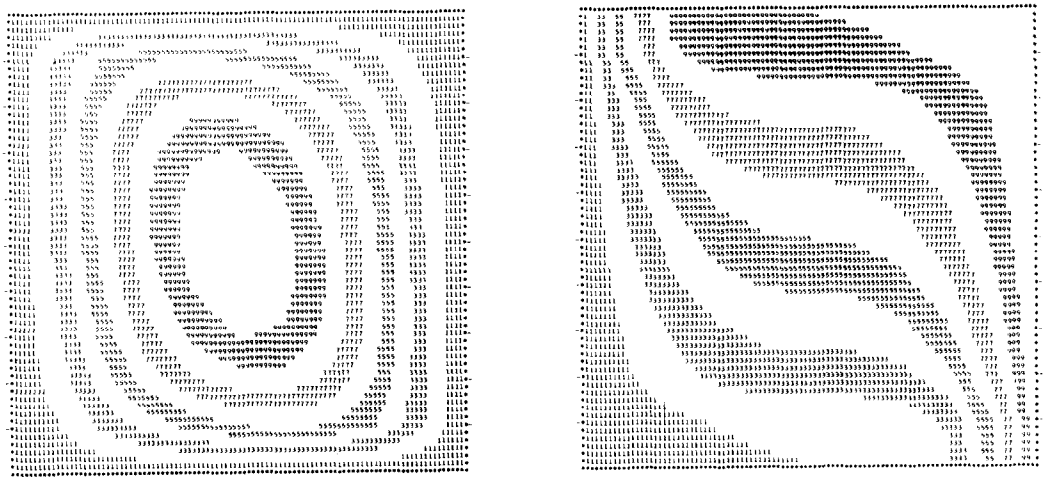

(b)

FIG. 4. Contour maps of ψ and θ. $l/d = 5$. Insulated. (a) $Ra_l = 1{\cdot}25 \times 10^5$, $Pr = 10^3$. (b) $Ra_l = 1{\cdot}25 \times 10^6$, $Pr = 10^3$.

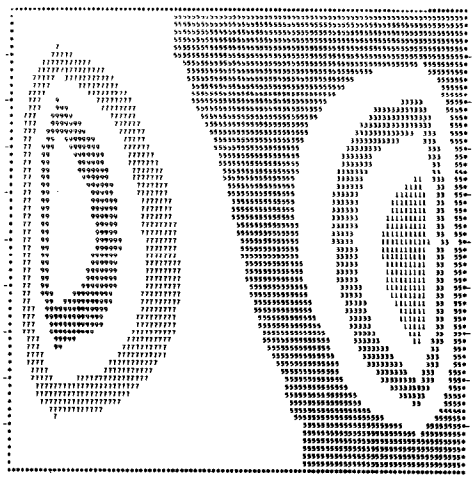

(a)(i)

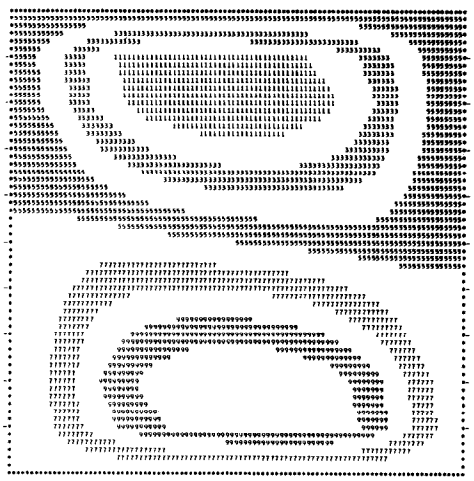

(a)(ii)

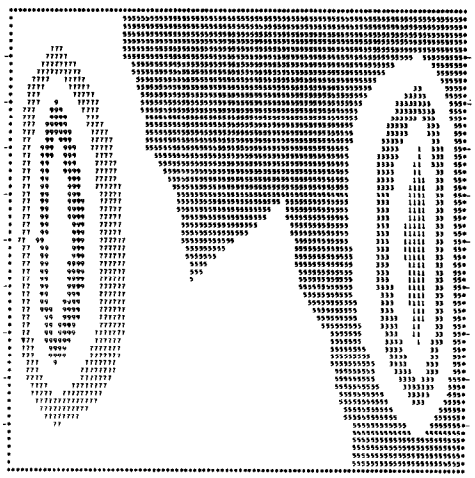

(b)(i)

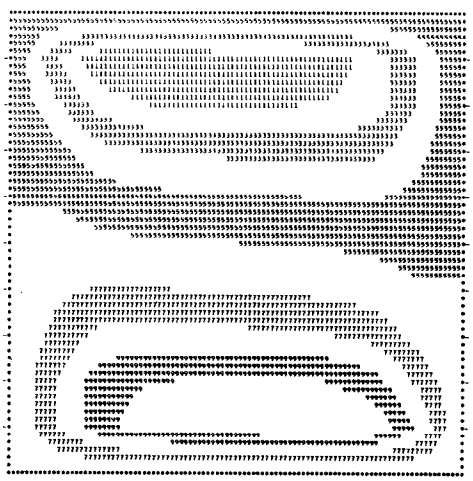

(b)(ii)

FIG. 5. Contour maps of u and v. $l/d = 1$. Linear. (a) $Ra = 2 \times 10^4$, $Pr = 10^3$; (i) u-component (ii) v-component. (b) $Ra = 10^5$, $Pr = 10^3$; (i) u-component (ii) v-component.

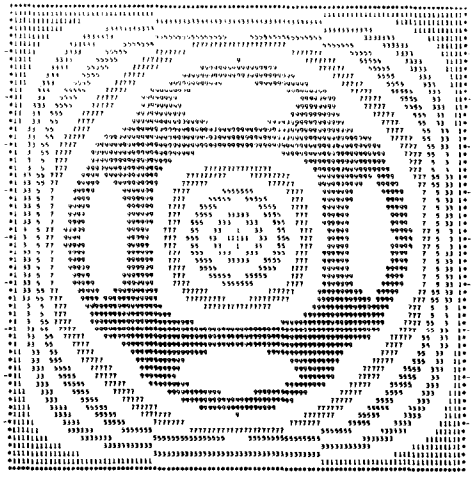

(a)

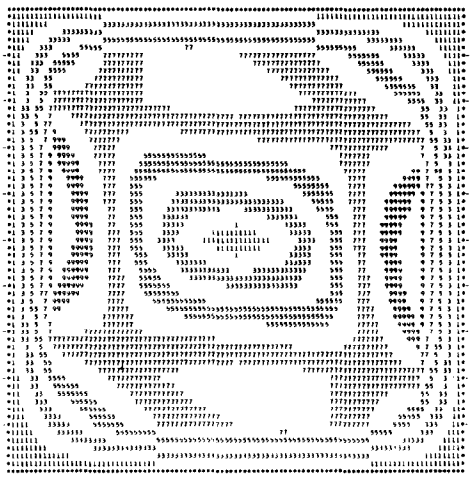

(b)

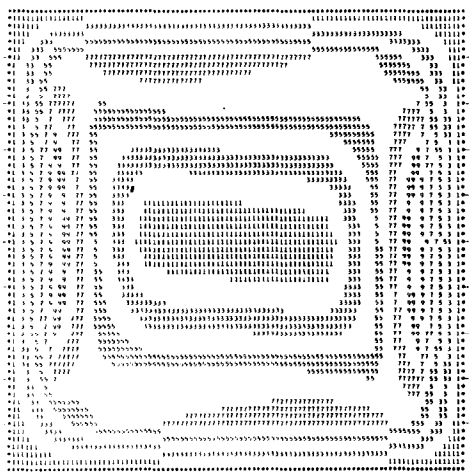

(c)

FIG. 6. Contour maps of fluid speed $(u^2 + v^2)^{\frac{1}{2}}$. $l/d = 1$, linear. (a) $Ra = 10, Pr = 10$ (b) $Ra = 2 \times 10^4$, $Pr = 10^3$ (c) $Ra = 10^5$, $Pr = 10^3$.

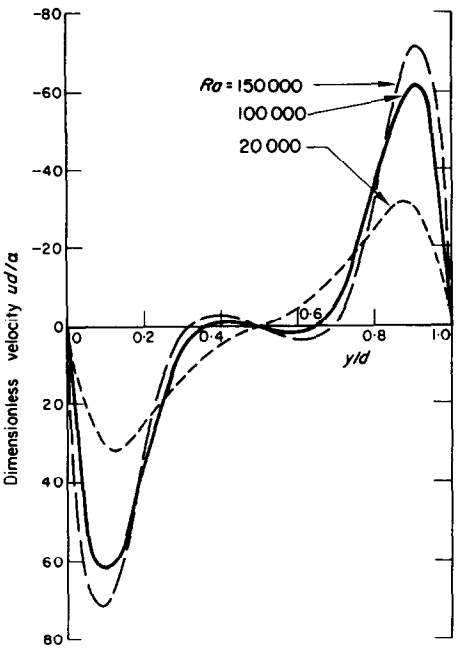

FIG. 7. Vertical velocity component at mid-height of cavity. $l/d = 1$, linear

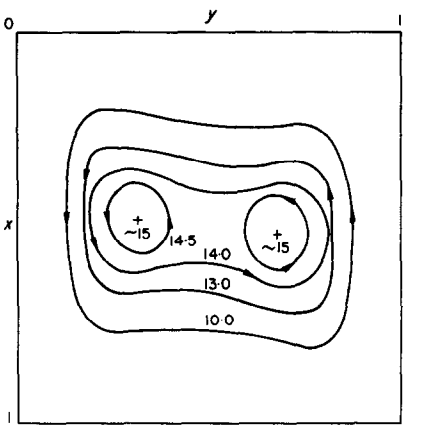

FIG. 8. Streamlines at large Rayleigh numbers, showing the double eddy. $Ra = 1{\cdot}5 \times 10^5$, $Pr = 10^3$, $l/d = 1$, linear.

Rayleigh numbers. This phenomenon was observed by Elder [1] and by Martini and Churchill [6]. It is predicted by Elder's approximate analysis. The streamline distribution is shown in Fig. 8.

When the reversal of motion was first observed in these computations, it was suggested to me that it might have been a consequence of trying to fit a 7-point approximation (as was being used at the time) to a curve which was essentially straight in the central region of the cavity. However, repetition of the calculations using 5- and 3-point formulae revealed the same effect. (Figures 7 and 8 are taken from the 3-point results.)

It seems that, at sufficiently high *Ra*, the boundary-layer flow is so well established that the strong vorticity near the walls is able to sustain a weak return motion in the outer part of the boundary layer and that, in this region of return flow (near the mid-height of the cavity), the opposite boundary layer is less able to influence this flow.

(c) *Temperature distribution*

Following Eckert and Carlson [15], the temperature distribution in the cavity has been used to distinguish between three regimes of flow. These are illustrated in Fig. 9, which shows the temperature distribution across the cavity, at the mid-height, for several values of Rayleigh number.

At the lowest *Ra* (below about 3000), the temperature profile is virtually linear; the flow of heat across the cavity under these conditions is due almost entirely to conduction. As *Ra* increases, convection becomes increasingly significant, and the profiles show a progressive departure from linearity. This is the transition regime. The horizontal temperature gradient becomes smaller, showing that the amount of heat crossing the cavity directly by conduction is diminishing.

Above $Ra \sim 10000$ the horizontal gradient of temperature becomes negative. The flow, now in the boundary-layer regime, is so strong that hot fluid has been carried over to the cold side of the cavity, and *vice versa*. Conduction in the central portion of the cavity is actually opposite to the overall direction of heat flow; there is very little convection in this region, the fluid motion being essentially vertical.

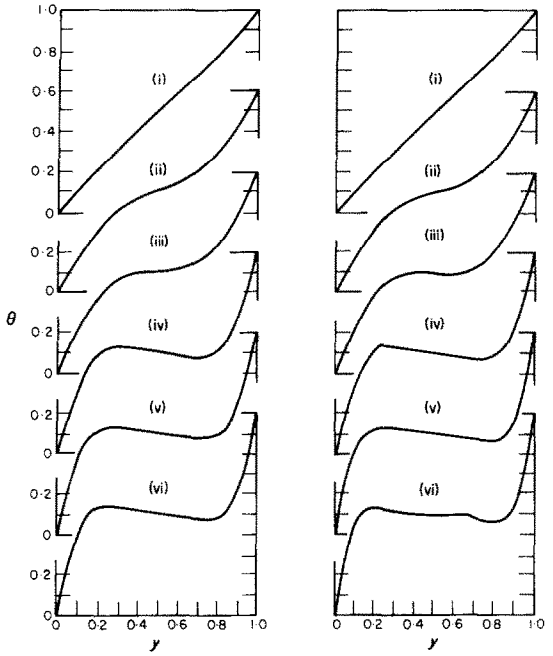

FIG. 9. Temperature distribution at mid-height of cavity. $l/d = 1$. $Pr = 10^3$. (a) Linear, 7-pt. (b) Insulated, 3-pt. (i) $Ra = 10^3$ (ii) 5×10^3 (iii) 10^4 (iv) 5×10^4 (v) 10^5 (vi) $1{\cdot}5 \times 10^5$

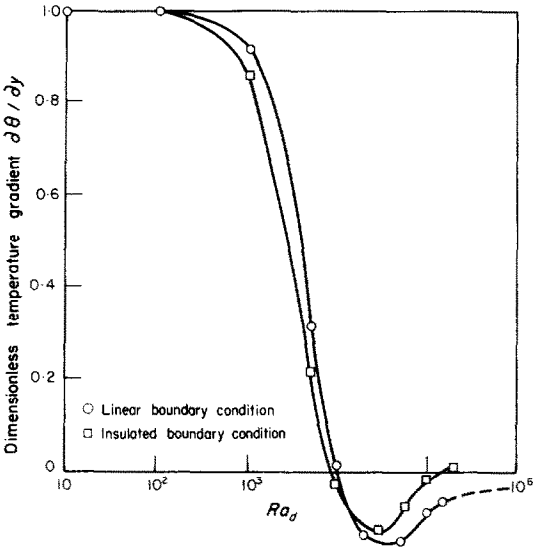

FIG. 10. Horizontal temperature gradient at the cavity mid-point. $l/d = 1{\cdot}7$-pt.

Some details of the variation of the horizontal temperature gradient at the mid-point of the cavity are presented in Fig. 10. This gradient reaches a minimum at $Ra \sim 35000$ and appears to be approaching an asymptotic value of zero. The behaviour is similar for both thermal boundary conditions.

The vertical temperature gradient has a more complex behaviour. Figure 11 shows the value of this quantity at the mid-point of the cavity, as a function of Rayleigh number. Three regimes can again be distinguished. At low Ra, when the motion is in the conduction regime, the vertical gradient is essentially zero. As the fluid passes through the transition regime, the gradient increases. Once the flow enters the boundary-layer stage, the vertical temperature gradient experiences an oscillation with increasing Ra which appears to be converging. The final values will differ for the two boundary conditions (and may also depend upon l/d).

(d) *Effect of Prandtl number*

One of the interesting outcomes of these calculations has been an expression of the effect of the Prandtl number of the fluid on the motion—or, more precisely of its lack of effect. Table 1 lists some parameters of interest, as functions of Pr, for several values of Rayleigh number (the values given for ψ and $\partial\theta/\partial y$ are for the mid-point of the cavity).

On the other hand Pr was found to have a

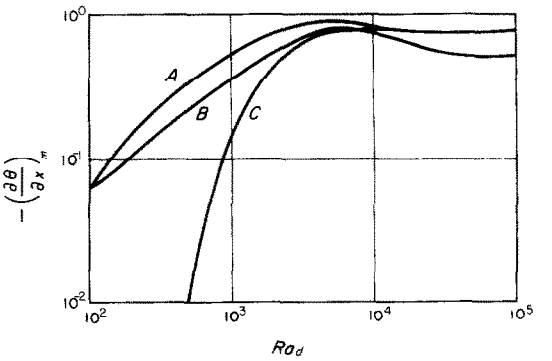

FIG. 11. Vertical temperature gradient at the cavity mid-point. (A) l/d, insulated, 3-pt. (B) $l/d = 1$, linear, 5-pt. (C) $l/d = 5$, insulated, 3-pt.

Table 1. Prandtl number effects

Ra	Pr	Nu	ψ_m	$(\partial\theta/\partial y)_m$	Conditions
1000	1000	1·033	1·186	0·916	l/d = 1, 5-pt.,
	10	1·033	1·186	0·916	linear
	0·1	1·033	1·171	0·913	
10000	1000	1·765	6·391	0·024	l/d = 1, 3-pt,
	10	1·767	6·380	0·023	linear
	0·733	1·773	6·249	0·005	
50000	1000	4·103	6·781	−0·067	l/d = 1, 7-pt,
	10	4·075	6·726	−0·066	insulated
	1	3·845	6·258	−0·060	
100000	1000	5·927	8·414	−0·021	l/d = 1, 3-pt,
	100	5·926	8·412	−0·020	insulated
	10	5·911	8·357	−0·017	
	1	5·723	7·786	−0·005	
150000	1000	6·717	8·848	0·003	l/d = 1, 3-pt,
	100	6·715	8·842	0·004	insulated
	10	6·698	8·790	0·006	
	1	6·499	8·191	0·019	

vital effect on the stability of the solution procedure, especially at the larger values of Ra. It was necessary to solve first for a large Pr—usually 1000—before stable solutions for lower Pr could be obtained.

This behaviour becomes explicable when the relative magnitudes of the two terms—inertia and buoyancy—in the vorticity transport equation (5) are compared. Figure 12 shows contour maps of these two terms, for two combinations of Ra and Pr.

At large Pr, and thus small Gr, the non-linear inertia term becomes negligible. The instabilities, which characteristically arise from non-linearities, are thereby suppressed. Once a solution has been obtained for large Pr, this provides a sufficiently good approximation to enable stable solutions to be found for lower Pr. Typically, rapid convergence was obtained for successive values of 100, 10, 1 and 0·1.

The fact that the term containing Pr in the equations is negligible except at very low values of Pr also explains the small effect Pr has on the numerical results obtained in the solution. Because of the smallness of the effect, many of the results given are for Pr = 1000, lower values having not been considered. The effect of Pr, however, increases as Ra increases, and is not negligible for $Ra > 5 \times 10^4$, as Table 1 shows.

(e) *Comparison with previous results*

Figure 13 shows the values of ψ at the midpoint of the cavity as a function of Rayleigh number. The agreement between the present results and those of Wilkes and Poots is excellent, for the linear thermal boundary condition. Further comparison is provided in Table 2, which includes some values of the mean Nusselt number.

For the insulated thermal boundary condition, a comparison with the results of Wilkes

Table 2. A comparison with some previous results—linear boundary condition—3 point formula

Ra		Author	Poots	Wilkes
1000	Nu	1·0410	1·041(8)	n.a.
5000	ψ_m	4·3157	4·3*	4·31
	Nu	1·4191	1·41(5)	1·419
10000	ψ_m	6·2492	6·2†	n.a.
	Nu	1·7735	1·70(6)	n.a.

* Calculated by Wilkes from Poots' equations.
† Estimated from a ψ-map published by Poots.

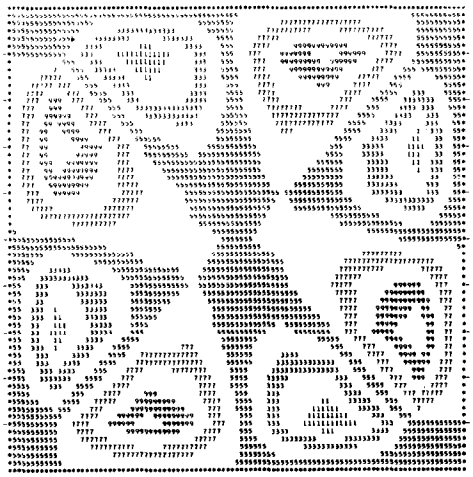

(a)(i)

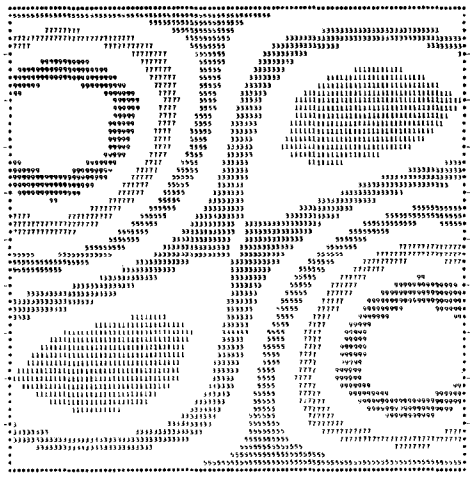

(a)(ii)

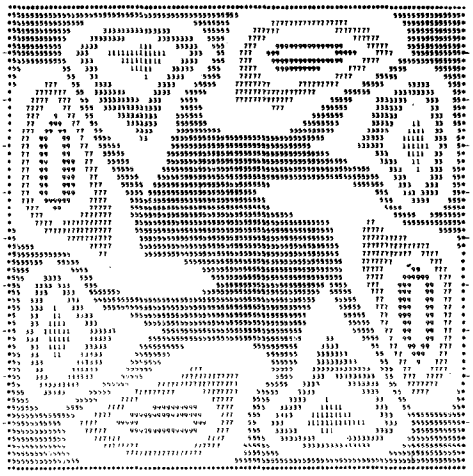

(b)(i)

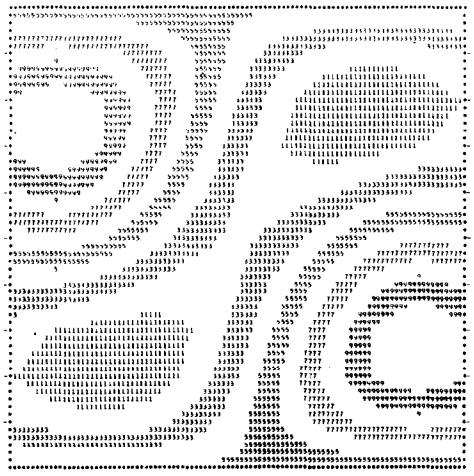

(b)(ii)

FIG. 12. Contour maps showing the distribution and relative magnitude of the inertia and buoyancy terms in the vorticity transport equation. (a) $Ra = 10^3$, $Pr = 10^3$ (i) Inertia-maximum = 0·184 (ii) Buoyancy-maximum = 0·121 $\times$ 10^4. (b) $Ra = 10^3$, $Pr = 10^{-1}$ (i) Inertia-maximum = 0·155 $\times$ 10^4 (ii) Buoyancy-maximum = 0·121 $\times$ 10^4.

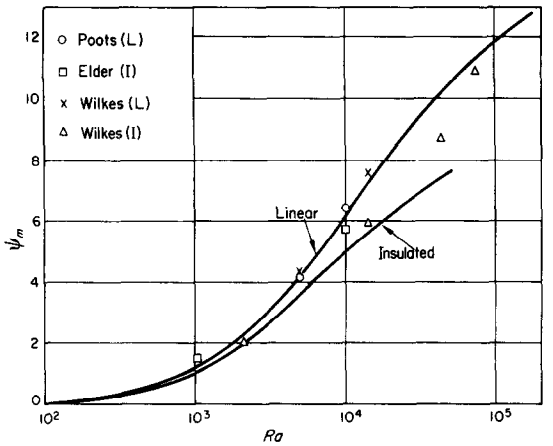

FIG. 13. Stream function at the cavity mid-point, as a function of Rayleigh number, compared with previous solutions.

and of Elder is less favourable. Elder's results differ appreciably from the present figures. In a test of the accuracy of his method [on the equation $\nabla^4(\psi/Ra) = 1$], errors of up to 35 per cent in ψ_{max} and 88 per cent in vorticity were reported. He attributed this to the vorticity boundary condition adopted—that its normal gradient should vanish on the horizontal boundaries—and presumably this condition led to errors of similar magnitude in the solution of the full equations. The form of his solution is in general agreement with that now and previously found, but his numerical values must be of limited accuracy.

Wilkes' values for ψ_m show a progressive departure from the present curve as Ra increases. The maximum Ra at which he was able to obtain a stable solution was 73300. This solution, however, is not acceptable because of the temperature distribution found is physically impossible (θ at a particular mesh point was higher than at the four surrounding mesh points). Wilkes suggested that, since this occurred adjacent to a boundary, it was likely to be due to a difficulty in specifying the vorticity boundary condition. If this is so, the error, although not apparent on inspection, may have been present to a lesser extent at lower values of Ra.

(f) *Heat-transfer results*

The parameters of practical importance are the heat-transfer coefficient and the Nusselt number (although the values of l/d considered so far are somewhat outside the range of interest).

The local heat-transfer coefficient h_x on a vertical boundary is defined by the following equivalent expressions for the heat flux, viz.

$$k\left(\frac{\partial T}{\partial y'}\right)_0 = \frac{k}{d}\left(\frac{\partial \theta}{\partial y}\right)_0 (T_h - T_c) = h_x(T_h - T_c).$$

Thus a dimensionless local heat-transfer coefficient can be defined as

$$\frac{h_x d}{k} = \left(\frac{\partial \theta}{\partial y}\right)_0.$$

The distribution along the boundary $y = 0$ of this quantity is shown in Fig. 14 for three different configurations and several values of Rayleigh number.

In Fig. 14(a) $(\partial\theta/\partial y)_0$ is constrained to the value unity at $x = 0$ and $x = 1$ by the boundary conditions there. This constraint has an influence on the heat-transfer coefficient for all x, the values in Fig. 14(b) being appreciably greater except near $x = 1$, where $(\partial\theta/\partial y)_0 \sim 0{\cdot}5$.

An average Nusselt number is defined by

$$Nu = \frac{\bar{h}l}{k} = \int_0^{l/d} \left(\frac{\partial \theta}{\partial y}\right)_0 \mathrm{d}x.$$

At low Ra, when $(\partial\theta/\partial y)_0 \to 1$ for all x, $Nu \to l/d$. Figure 15 shows the results of a numerical integration for Nu, together with some values obtained by others. In this and the following figure, the Rayleigh number is based upon l, on the grounds that over most of the Ra range the flow is of a boundary-layer nature, with l the significant length scale for the *average* heat-transfer rate.

The most noticeable feature of the present results is their variation with the finite difference approximation used, a variation more apparent in the heat-transfer result than in any other. This is doubtless due to the fact that the less

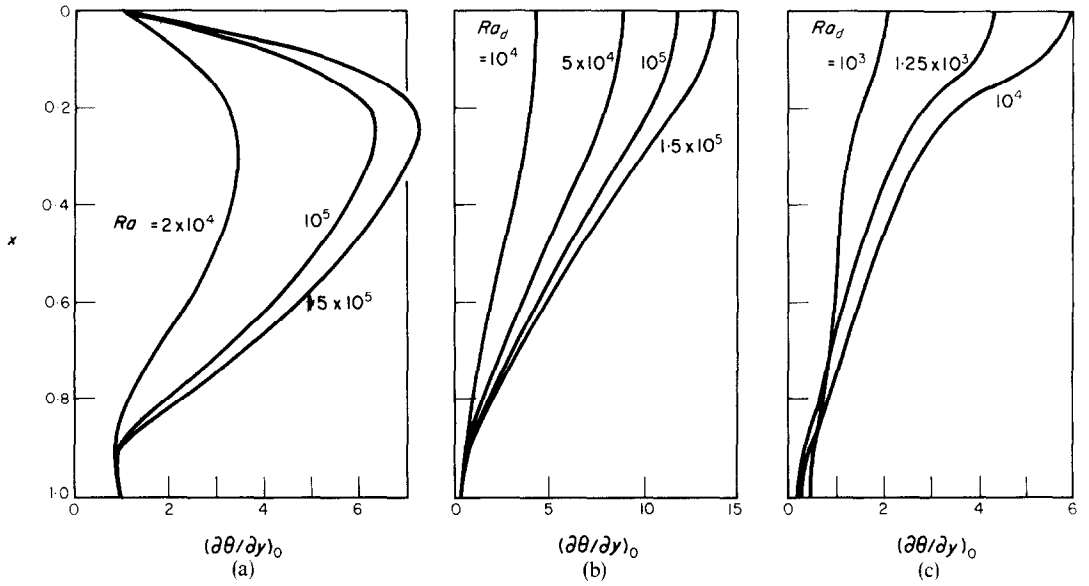

FIG. 14. Local heat-transfer coefficient at the cold boundary. (a) $l/d = 1$, linear, 3-pt. (b) $l/d = 1$, insulated, 3-pt. (c) $l/d = 5$, insulated 3-pt.

accurate forward difference approximation must be used to obtain the temperature gradient at the boundary, and that consequently the high order approximations allow values of θ deep in the interior to affect the wall gradient. It is again seen that the 3-point formula yields results in good agreement with those of Wilkes and Poots, but not of Elder.

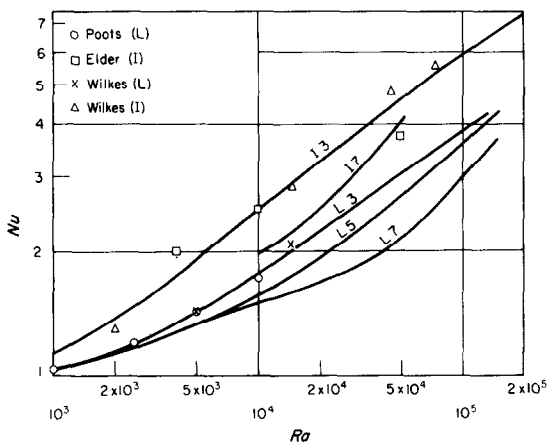

FIG. 15. Average Nusselt number for the square cavity, as a function of Rayleigh number, compared with previous solutions.

A comparison with the mass of experimental Nusselt number correlations which have been developed is somewhat irrelevant, since these are for l/d ratios of the order of ten to fifty. Under these conditions, the effects of the end regions become almost negligible, whereas here they predominate. Nevertheless, a few of these correlations, and the present results for $l/d = 5$, are shown on Fig. 16, together with the L3 and I3 curves from Fig. 15.

It is seen that the computed curves lie generally above the experimental curves, as is to be expected from the increased importance of the end regions. The curve for $l/d = 5$ (insulated boundary condition) lies below I3 curve ($l/d = 1$) for the same reason. The rapid increase in the slope of the former curve is associated with the transition from conductive to convective heat transfer, which Eckert and Carlson observed to occur at $Ra \sim 2 \times 10^5$ for $l/d = 5$.

For the reasons already stated, it would not be meaningful to generalize on the $Nu - Ra$ relationships so far revealed. The most that should be said is that the discrepancies between these and the measured figures are capable of plausible explanation. To say more, we need

both experimental data for small l/d, and further computation for large l/d. The latter, incorporating a refined mesh structure, is now in progress.

CONCLUSION

It has been shown that a stable numerical solution of the vorticity transport and energy equations can be obtained for values of Rayleigh number up to 2×10^5 (in a square cavity). Convergence of the solution has been demonstrated indirectly by comparison with previous results. The role played by the Prandtl number, both as a stabilizing factor and in its effect on the results, has been revealed. The lines of research to be pursued now include (a) use of a finer mesh to re-examine the convergence of the solution, (b) use of a graduated mesh (smaller mesh size near $x = 0$ and $x = l/d$) which will enable solutions for large l/d to be obtained without necessitating a prohibitive amount of computation, (c) examination of alternative boundary conditions, in particular a specified heat flux (rather than temperature) on $y = 0$ and $y = 1$, and (d) incorporation of internal heat generation in the fluid.

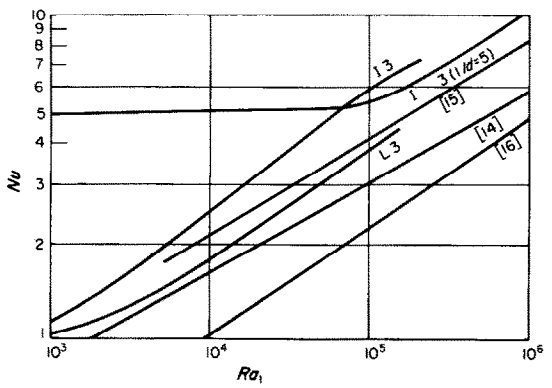

FIG. 16. Average Nusselt number compared with some empirical correlations.

ACKNOWLEDGEMENTS

This work was carried out in part at the University of New South Wales, with the financial support of the Australian Atomic Energy Commission; and in part at New York University, with the support of NASA Contract NGR-33-016-067. The work was completed at Brown University, with the support of NSF Grants GK-1305 and GP-4825.

I am grateful to New York University and Brown University for having made possible my visits there, to their computing centres for their assistance, and in particular to Professor Fred Landis of N.Y.U. for the benefits of many valuable discussions.

REFERENCES

1. J. W. ELDER, Laminar free convection in a vertical slot, *J. Fluid Mech.* **23**(1), 77–98 (1965).
2. G. K. BATCHELOR, Heat transfer by free convection across a closed cavity between vertical boundaries at different temperatures, *Q. Appl. Math.* **12**(3), 209–233 (1954).
3. H. BÉNARD, Les tourbillons cellulaires dans une nappe liquide transportant de la chaleur par convection en régime permanent, *Ann. Chim. Phys.* **23**, 62 (1901).
4. G. POOTS, Heat transfer by laminar free convection in enclosed plane gas layers, *Q. Jl Mech. Appl. Math.* **11**(3), 257–273 (1958).
5. J. D. HELLUMS and S. W. CHURCHILL, Transient and steady state, free and natural convection, numerical solutions. *A.I.Ch.E. Jl* **8**, 690–695 (1962).
6. W. R. MARTINI and S. W. CHURCHILL, Natural convection inside a horizontal cylinder, *A.I.Ch.E. Jl* **6**(2), 251–257 (1960).
7. E. R. MENOLD and S. OSTRACH, Natural convection in a horizontal cylinder at large Prandtl numbers, Report No. FTAS/TR-65-4, Engineering Division, Case Institute of Technology, Cleveland, Ohio (1965).
8. J. O. WILKES and S. W. CHURCHILL, The finite difference computation of natural convection in a rectangular enclosure, *A.I.Ch.E. Jl* **12**, 161–166 (1966).
9. J. O. WILKES, The finite difference computation of natural convection in an enclosed rectangular cavity, Ph.D. Thesis, University of Michigan (1963).
10. K. AZIZ and J. D. HELLUMS, Numerical solution of the three-dimensional equations of motion for laminar natural convection, *Physics Fluids* **10**(2), 314–324 (1967).
11. J. W. ELDER, Numerical experiments with free convection in a vertical slot, *J. Fluid Mech.* **24**(4), 823–843 (1966).
12. G. DE VAHL DAVIS and C. F. KETTLEBOROUGH, Natural convection in an enclosed rectangular cavity, *Trans. Inst. Engrs, Australia* **MC1**, 43–49 (1965).
13. G. DE VAHL DAVIS, Laminar natural convection in a rectangular cavity, Report No. F-67-2, School of Engineering and Science, New York University, N.Y. (1967).
14. F. LANDIS and H. YANOWITZ, Transient natural convection in a narrow vertical cell, in *Proceedings of the Third International Heat Transfer Conference*, Am. Inst. Chem. Engrs, New York (1966).
15. E. R. G. ECKERT and W. O. CARLSON, Natural convection in an air layer enclosed between two vertical plates with different temperatures, *Int. J. Heat Mass Transfer* **2**, 106–120 (1961).

16. D. DROPKIN and E. SOMERSCALES, Heat transfer by natural convection in liquids confined by two parallel plates which are inclined at various angles with respect to the horizontal, *J. Heat Transfer* **87**, 77–84 (1965).
17. R. W. THOMAS, Private communication, Research student, University of New South Wales.
18. W. G. BICKLEY, Formulae for numerical differentiation, *Mathl Gaz.* **25**, 19–27 (1941).

APPENDIX

The solution of equations (5) and (6) involves their reduction, in turn, to sets of eighty-one or ninety-nine finite difference equations. Derivatives are replaced by central difference formulae at all points except those on or near boundaries.

Suppose (for the purpose of this paragraph) that the cavity is square and is divided into a 5×5 mesh (i.e. $h = \frac{1}{4}$). If (DX) is a matrix defined by

$$(DX) = \frac{1}{2h}\begin{bmatrix} -3 & 4 & -1 & 0 & 0 \\ -1 & 0 & 1 & 0 & 0 \\ 0 & -1 & 0 & 1 & 0 \\ 0 & 0 & -1 & 0 & 1 \\ 0 & 0 & 1 & -4 & 3 \end{bmatrix}$$

then the result of the matrix multiplication $(DX) \times (\psi)$ is a matrix of which the elements are three-point finite difference approximations to $\partial\psi/\partial x$. Similarly, an approximation to $\partial\psi/\partial y$ is obtained from $(\psi) \times (DX)^T$. The non-linear terms in (5) and (6) are obtained by term-by-term operations on the respective elements of the relevant matrices. In this manner, (5) and (6) are replaced by

$$\nabla^4\psi = (\text{RHS}\psi) \tag{A.1}$$

and

$$\nabla^2\theta = (\text{RHS}\theta), \tag{A.2}$$

where the right-hand sides in (A.1) and (A.2) are matrices.

Equation (A.1) is now written as

$$(\text{DEL4}) \times (\psi) = (\text{RHS}\psi) \tag{A.3}$$

where (DEL4) is in fact an 81×81 matrix, there being eighty-one internal (unknown) values of ψ when using a 10×10 mesh, and where (ψ) and $(\text{RHS}\,\psi)$ are now column vectors, the elements of which are taken from the respective matrices in row order for convenience. The elements of (DEL4) are such that the left hand side of (A.3) provides a finite difference approximation to $\nabla^4\psi$ at each of the eighty-one internal points. The boundary conditions on ψ and its derivatives are incorporated into the construction of (DEL4).

Since the elements of (DEL4) are independent of the problem parameters (Ra and Pr), (A.3) is most readily solved by

$$(\psi) = (\text{D4INV}) \times (\text{RHS}\psi)$$

where (D4INV), the inverse of (DEL4), need only be computed once. (The inversion of the 81×81 matrix required about 1·9 s of CDC 6600 time.)

When $\nabla^2\theta$ is replaced by a finite difference approximation, (A.2) becomes

$$(\text{DEL2}) \times (\theta) = (\text{RHS}\theta). \tag{A.4}$$

The elements of (DEL2) are, however, functions of ψ and the solution of (A.4) by inversion is impractical. Instead, successive over-relaxation is used, the relaxation factor being chosen (automatically) to keep the number of iterations to a minimum. In fact, due no doubt to the non-linearities in (6), the relaxation factor is always less than one, and the method is more properly termed under-relaxation. Thus (A.4) is solved at all internal points and, if the horizontal boundaries are specified to be adiabatic, equation (7b) is used to extrapolate to new values of θ at $x = 0$ and $x = l/d$.

Résumé—On décrit une étude du mouvement bidimensionnel laminaire et permanent d'un fluide dans une cavité fermée, le mouvement étant engendré par un gradient de température normal à la direction de la force volumique. Les équations qui régissent ce mouvement ont été résolues numériquement. Les résultats sont compatibles avec quelques résultats théoriques et expérimentaux antérieurs et en constituent une extension. Les valeurs maximales du nombre de Rayleigh (basé sur la hauteur de la cavité) qui ont été

considérées étaient de 2×10^5 pour une cavité carrée et de $1{,}25 \times 10^6$ pour une cavité dont le rapport de la hauteur sur l'épaisseur était égal à 5. Quelques nouveaux détails de l'écoulement à des nombres de Rayleigh élevés ont été découverts. On a trouvé que des nombres de Prandtl élevés exercent une influence stabilisatrice sur la solution numérique, tandis qu'ils ont seulement un effet faible sur les résultats finaux (dans la gamme $10^{-1} \leqslant Pr \leqslant 10^3$).

Zusammenfassung—Es wird von einer Untersuchung berichtet über stationäre, laminare, zweidimensionale Flüssigkeitsbewegungen in einem Hohlraum. Die Bewegung wird von einem Temperaturgradienten senkrecht zur Richtung der Massenkraft hervorgerufen. Die charakteristischen Gleichungen wurden numerisch gelöst. Die Ergebnisse sind vergleichbar mit einigen theoretischen und experimentellen Resultaten und bilden deren Erweiterung. Die Maximalwerte der betrachteten Rayleigh–Zahlen (gebildet mit der Hohlraumhöhe) betrugen 2×10^5 für einen quadratischen Hohlraum und $1{,}25 \times 10^6$ für einen Raum vom Höhen-Breiten-Verhältnis 5. Einige neue Einzelheiten der Strömung bei hohen Rayleigh–Zahlen waren zu erkennen. Es zeigte sich, dass hohe Prandtl–Zahlen einen stabilisierenden Einfluss auf die numerische Lösung ausüben, während sie nur einen geringen Einfluss auf die Endergebnisse haben (im Bereich $10^{-1} \leqslant Pr \leqslant 10^3$).

Аннотация—Описывается стационарное ламинарное двухмерное движение жидкости в замкнутой полости, причем движение происходит за счет температурного градиента по нормалли к направлению массовой силы. Численно решены основные уравнения. Результаты сравниваются с ранее полученными теоретическими и экспериментальными данными. Максимальные значения числа Релея (построенного по высоте полости) составляют 2×10^5 для квадратной полости и $1{,}25 \times 10^6$ для отношения высоты к толщине 5:1. Обнаружены некоторые новые особенности течения при больших числах Релея. Найдено, что большие числа Прандтля все время влияют на численное решение, в то время как они незначительно сказываются на конечных результатах (в диапазоне $10^{-1} \leqslant pr \leqslant 10^3$).